MACDCB: Design of an Efficient Multidomain Augmentation Model for Cloth Defect Identification via Cascaded Binary Classifiers

Girish Patil[1]*, Dr. S. M. Deshmukh[2]
[1]*PhD Scholar, Prof. Ram Meghe Institute of Technology & Research, Badnera*, patilgirish213@gmail.com
[2]*Professor & Head, Prof. Ram Meghe Institute of Technology & Research,Badnera*, smdeshmukh001@yahoo.com

Abstract: Cloth defect identification is a multidomain task that involves pre-processing of cloth image samples, segregation of samples into window-based patches, representation of these samples into multimodal feature sets, and classification of these feature sets into one-of-N defect categories. Existing deep learning models for cloth-defect identification are inefficient due to unavailability of data samples, and use of non-binary classifiers. Moreover, the scalability of these models is also limited, because accuracy of classification reduces w.r.t. increase number of cloth defect classes. To overcome these issues, this text proposes design of an efficient multidomain augmentation model for cloth defect identification via cascaded binary classifiers. The proposed model initially performs context-specific augmentation of cloth-defect samples in order to generate rotated, tilted, zoomed, shifted, and brightness modified images. These modifications are done such that correlation between images of same category is maximum, while correlation between images of distinctive categories is maximum, which assists the classifier(s) to identify images with higher efficiency levels. These classifiers consist of a Cascaded arrangement of binary Convolutional Neural Networks (CabCNNs), each of which is capable of classifying the augmented image sets into 'single defect' or 'no defect' categories. The 'single defect' categories include 'Bad Selvage', 'Holes', 'Oil Spot', 'Thickness Defect', and 'Broken Ends' classes. The CabCNNs process converges if test image is categorized into a 'single defect' class. If the process is not converged, then test image is categorized into 'no defect' class. Due to this process, the model is able to categorize input images with over 98.5% accuracy, which is 3.5% higher than existing models. It is also observed that the proposed model is able to achieve 2.9% higher precision, and 3.2% higher recall with 1.8% lower delay when compared with existing models under similar defect image sets.

Keywords: Cloth Defect, Multidomain Augmentation, Cascade Convolutional, Neural Networks, binary,etc

1. Introduction

An important part of any quality control procedure for fabrics is the detection of flaws in the material. Because of these flaws, the cost of the cloth might drop by as much as 65% [1, 2, 3, 4]. These flaws can be detected via Activation Layer Embedded Convolutional Neural Network (ALE CNN), and other deep network techniques. Manual work or operation is usually the backbone of any inspection system. As the cloth is being moved by a machine, they must spot any flaws. These powered systems use standard methods to unwind fabric rolls, elongating the fabric and delivering it to the worker wrinkle- and thickness variation-free. Due to the high dependency on one's eyesight and level of focus required, this task may prove to be exceedingly monotonous and time-consuming, eventually leading to human mistake. This means that older systems, despite their slower output rate, can only achieve an accuracy of 60% to 75%. This means that automated visual inspection systems are becoming more necessary to guarantee the highest quality goods on assembly lines. Instead of relying on subjective human judgment, automated defect detection systems provide many key benefits [5, 6] which propose use of multitask mean teacher (MT) along with augmented network sets. Investment in automated fabric inspection systems is economically viable, according to study in [7], when classification delays are kept to a minimum and related advantages are included in. There are several challenges to be solved despite the many benefits of automated visual inspection systems. Numerous instances [8, 9, 10] provide significant challenges that are solved viaStacked De-noising Convolutional Auto-Encoder (SDCAE)and other deep learning methods, because to the large number of features, interclass similarity, and intraclass variability of fabric flaws.

The autocorrelation function, eigen filters, histogram, Gray Level Co-occurrence Matrix (GLCM), Local Binary Patterns (LBP), mathematical morphology, and fractal dimension are all major methods of statistics. This category of methods investigates the statistical relationships between grayscale picture levels. When comparing the statistical qualities of the problematic fabric and the defect-free areas, the latter stands out since it is not statistically consistent over a large percentage of the inspection photos. Most of these methods are only useful for fixing certain kinds of defects and need background information on how a perfect system operates. According to the research in [11, 12, 13, 14], the autocorrelation function was used to characterize and evaluate the symmetry of carpet fabric patterns via CNNs. Using eigen-filter data, a study in [15, 16, 17] successfully located flaws in textured materials with a minimal false alarm rate.

Research [18, 19, 20] suggested using rotationally, negation-wise, and mirror-symmetrically crafted eigen filters for texture fault identification. Through the use of histogram equalization, noise filtering, and thresholding, [9] was able to identify issues with the fabric with an accuracy of 85%. The method was tested using a wide variety of well-known textures, including as wood patterns, and 14 unique criteria retrieved from the GLCM were discovered to assess texture features in [21]. In [22, 23, 24, 25], these characteristics were used to build a fault detection system that achieved a 95% accuracy rate over a wide range of problem types. Using a Support Vector Machine (SVM), the authors of [26] were able to accurately categorize a wide variety of problems to the tune of 80%. In the investigation reported in [13], LBP was used to compare test samples to fabric samples and identify those that did not have defects. With this method and an SVM, the researchers in [27] achieved an average accuracy of 86.7% in detecting damaged samples. In 2001, Work in [28] built a decision tree using morphologic operations and thresholding to find and categorize errors with 91.25 percent accuracy. In order to identify flaws in textiles, researchers [29, 30] developed morphological filters with a 96.7% accuracy rate. In order to identify flaws in textiles, research [17] created an inspection strategy based on the variation of fractal dimension. The researchers found that the technique's high false alarm rate and low defect localization accuracy resulted to detection rates of 96% for just eight defect types, despite the technique's apparent ease of use.

Many of the available statistical methods become useless when used to fabric flaws with particularly smooth transitions. This has led to the development of methods that are both more reliable and more effective. Textured pictures must exhibit a great deal of periodicity for spectral techniques to analyze them successfully in the spatial frequency domain. The Wavelet transform, Gabor filters, and iterative applications of the Fourier transform are all examples of such techniques. The flaws in fabrics were detected using the optical Fourier transform and a neural network [31]. Researchers in [32] explored a discrete Fourier transform and Hough transform combination to improve the image's difficult area. Using Gabor filters, [20] classified a number of faulty pattern textiles that had previously been recorded. In [21], a wavelet-based inspection system with a low false alarm rate (2.5%), a high accuracy rating (88%), and a cheap price of installation was developed. In [22], the authors develop a flaw detection strategy based on wavelet transform and fuzzy analysis. Using wavelet transform and principal component analysis, the team in [23] was able to classify thermal picture sets with a 95% success rate.

Image textures may be created using either a stochastic or deterministic approach with fixed parameters. Despite their huge complexity and significant computing price, these approaches could perform well for pictures with uneven patterns. These tactics combine the Gaussian Markov random field and the autoregressive model. Sometimes, the complexity and monetary burden of these models becomes prohibitive. Different fabric textures were generated using autoregressive models and compared in [24]. Researchers [25] used a Gaussian Markov random field model to represent flawless cloth, then compared this model to photographs of test fabrics to identify flaws.

The use of learning approaches has been facilitated by recent advancements in processing speed and data volume. These methods, which look for repeating structures in the recovered characteristics of a fabric picture, may be employed alone or in tandem with others, such as LBP [26] and GLCM [27]. This category covers algorithms such as Support Vector Machines [28], Feed-forward Networks (FFNs) [29], CNNs [31, 32], and others. In order to distinguish between three distinct varieties of fabric flaws, researchers at [23] devised an SVM-based inspection strategy. In the work detailed in [24], principal component analysis was used to lower the dimension of the characteristics vector, and it was combined with a two-layer FFN to build a trustworthy, low-cost defect detection system. Using a multi-scale convolutional denoising auto-encoder network and a Gaussian pyramid, the research in [25] created an automated, unsupervised learning-based approach for identifying and segmenting fabric problems. Their overall inspection accuracy was more than 80% across all datasets. Errors in a dataset developed by the authors were detected by a CNN with a success rate of 98.82%. It is important to note that several of the aforementioned methods have high defect detection accuracy rates, but are computationally inefficient. Taking into account a variety of material fault types could further degrade their accuracy. Weaknesses in existing deep learning models for fault detection in textiles stem from insufficient training data and the use of non-binary classifiers. Further, as the number of textile defect classes grows, the models' capacity to classify them accurately becomes increasingly constrained. As a solution to these challenges, the next portion of this research proposes the creation of an efficient multidomain augmentation model for recognizing textile faults through cascaded binary classifiers. In subsection 3, we compared the performance of the proposed model to that of similar current approaches using the same picture datasets. This article closes with context-specific remarks regarding the proposed model and proposals for further refining it for usage in real-world scenarios.

2. Design of an efficient Multidomain Augmentation model for Cloth Defect identification via Cascaded Binary classifiers

As per the review of currently used cloth defect identification techniques, it was observed that existing deep learning models for cloth-defect identification are inefficient due to unavailability of data samples, and use of non-binary classifiers. Moreover, the scalability of these models is also limited, because accuracy of classification reduces w.r.t.

increase number of cloth defect classes. To overcome these issues, this section discusses design of an efficient multidomain augmentation model for cloth defect identification via cascaded binary classifiers. Flow of the model is depicted in Fig 1, where it can be observed that the proposed model initially performs context-specific augmentation of cloth-defect samples in order to generate rotated, tilted, zoomed, shifted, and brightness modified images. These modifications are done such that correlation between images of same category is maximum, while correlation between images of distinctive categories is maximum, which assists the classifier(s) to identify images with higher efficiency levels. These classifiers consist of a Cascaded arrangement of binary Convolutional Neural Networks (CabCNNs), each of which is capable of classifying the augmented image sets into 'single defect' or 'no defect' categories. The 'single defect' categories include 'Bad Selvage', 'Holes', 'Oil Spot', 'Thickness Defect', and 'Broken Ends' classes. The CabCNNs process converges if test image is categorized into a 'single defect' class. If the process is not converged, then test image is categorized into 'no defect' class.

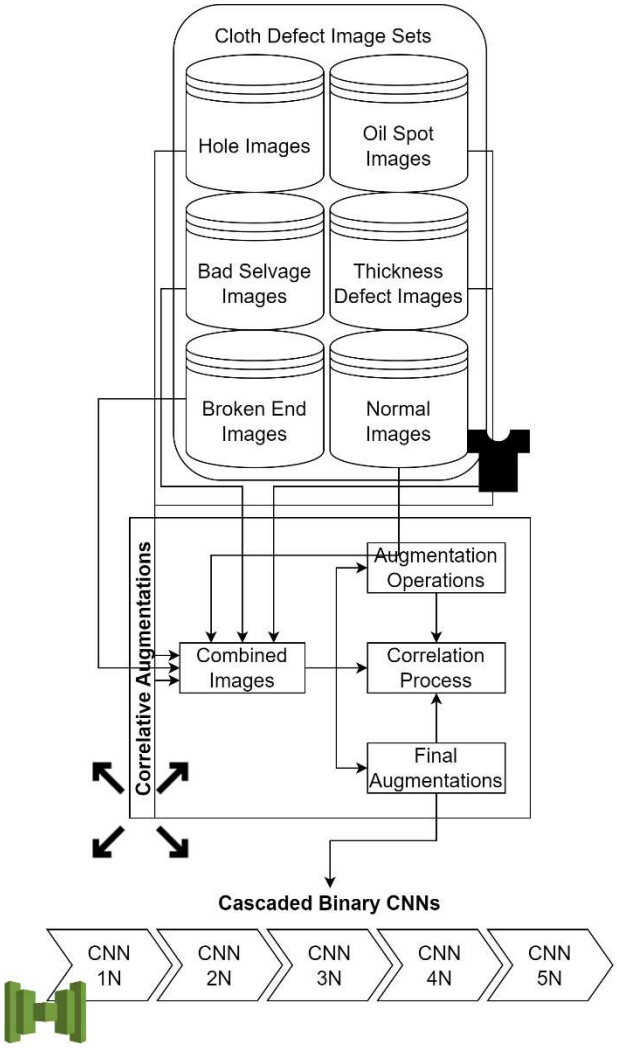

Fig. 1. Flow of the proposed cloth defect detection process

Based on the flow of proposed model, it can be observed that input images are initially augmented via a series of rotated, tilted, zoomed, shifted, and brightness operations. An example of these operations for 'Bad Selvage' images can be observed from figure 2, where a single image is augmented into 45 different variants, which assists in identification of high-density feature sets. These feature sets are evaluated via convolutional operations, but can result into feature-level redundancies due to similar augmentations. To reduce these redundancies, a correlation distance metric is evaluated between these features. This distance metric is estimated via equation 1, and uses cross-pixel distance metrics for estimation of similarities.

$$d(s_i, s_j) = \frac{1}{N * M} * \sum_{i=1}^{N_S} \sqrt{\sum_{r,c}^{N,M} \frac{(P_{i_r} - P_{j_r})^2 + (P_{i_c} - P_{j_c})^2}{Var(s_i, s_j)}} \dots (1)$$

Where, $s_i \& s_j$ are the augmented images between which correlation is being estimated, while Prepresents the pixel levels of these images, var represents variance of pixels between the images, N, M are the image dimensions, while N_s are number of augmentation samples used for analysis.

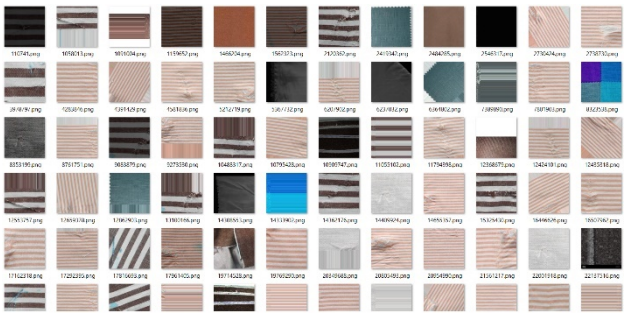

Fig 2. A sample of augmented images for 'Bad Selvage' defects

This distance is estimated for all augmented images that are generated from a single image, and then a distance threshold is estimated via equation 2,

$$d_{th} = \sum_{i=1}^{N_S} \sum_{j=1}^{N_S} \frac{d(s_i, s_j)}{N_S^2} \dots (2)$$

Images with $d > d_{th} * S_f$ are selected by the augmentation process, while others are discarded due to higher redundancies. In this case, S_f is a selection factor, which can be tuned to increase or reduce number of augmented images. These images are processed via a binary cascaded Convolutional Neural Network (CNN), that assists in classifying input images into 'defect' & 'non-defect' categories. Flow of the CNN Model is depicted in **Fig** 3, where different Convolutional Layers are connected with Max Pooling and Drop Out layers for identification of high-density feature sets. The convolutional layers use equation 3 to identify window-based features, which might induce feature-level redundancies.

$$Conv_{s_{i,j}} = \sum_{a=-\frac{m}{2}}^{\frac{m}{2}} \sum_{b=-\frac{n}{2}}^{\frac{n}{2}} I_s(i-a, j-b) * ReLU\left(\frac{m}{2} + a, \frac{n}{2} + b\right) \dots (3)$$

Where, m, nrepresents the window dimensions for image I_s, and a, b represents stride dimensions, which are varied as per the following **Fig** 3,

Due to a wide range of window sizes from 64x64 to 512x512, the model is able to estimate large number of features. These feature counts are represented via equation 4,

$$f_{out} = \frac{f_{in} + 2 * p - k}{s} + 1 \dots (4)$$

Where, f_{in}, f_{out} are the input and output features, while $p, k \,\&\, s$ are padding sizes, kernel sizes and stride sizes for different convolutional layers. As the number of features increases, the redundancy between these features also increases. To reduce this redundancy, a feature-level threshold is estimated via equation 5,

$$f_{th} = \left(\frac{1}{X_k} * \sum_{x \in X_k} x^{p_k}\right)^{\frac{1}{p_k}} \dots (5)$$

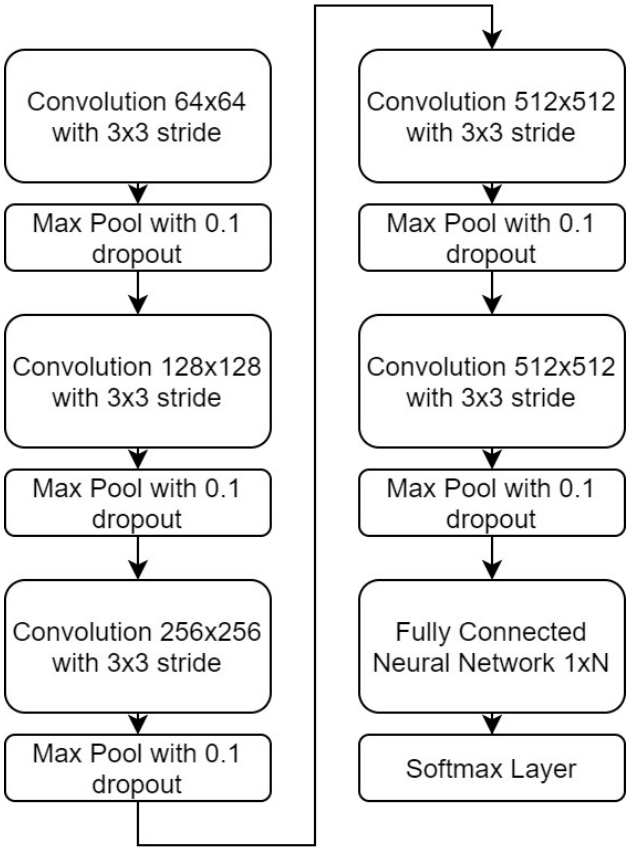

Fig 3. Design of the CNN Model for identification of 'defect' & 'non-defect' categories

This threshold is evaluated by the Max Pooling and Drop Out layers, where, X_k represents number of convolutional features, x represents their feature values, while p_k represents variance of these features. All features with $f > f_{th}$ are passed to next convolutional layers, while others are discarded from further convolutional operations. This process is repeated for each of the layers, and finally a Fully Connected Neural Network (FCNN) is used to identify defect classes. This FCNN uses SoftMax based activations in order to convert feature sets into 'defect' and 'non-defect' categories via equation 6,

$$c_{out} = SoftMax\left(\sum_{i=1}^{N_f} f_i * w_i + b_i\right) \dots (6)$$

Where, N_f represents number of extracted features by the convolutional layers, and w, b represents weights and biases of these features. The output class c_{out} is estimated via SoftMax activation, which assists in tuning the weights and biases for optimal classification performance under limited number of categories.

Such CNN Models are deployed for individual cloth defects, thus for N defects, $N-1$ CNNs are needed for efficient classification performance levels. Each of these CNNs are responsible for classification of images into single defect categories. The final class is estimated via equation 7 as follows,

$$c_{final} = Normal, if\ converge$$
$$else, \bigvee_{i=1}^{N_d} C_i \dots (7)$$

Where, N_d represents total number of defects, C_i is the defect category, while $\bigvee C$ represents the disease class. Based on this process, the model is able to identify different cloth defect classes with high efficiency levels. These efficiency levels were evaluated in terms of accuracy, precision, recall and delay values in the next section of this text.

3. Result Analysis & Comparison

The proposed model initially collects cloth images from different defect classes, and augments them via a correlation process. This correlation process assists in identification of highly un-correlative class-level image sets. These image sets are classified into 1 of N defect categories via a binary cascaded CNN process. Due to use of binary classification the model is able to estimate defect classes with high efficiency levels. These efficiency levels were estimated in terms of accuracy (A), precision (P), recall (R), and delay (d) metrics, via equations 8, 9, 10, and 11 as follows,

$$A = \frac{t_p + t_n}{t_p + t_n + f_p + f_n} \dots (8)$$

$$P = \frac{t_p}{t_p + f_p} \dots (9)$$

$$R = \frac{t_p}{t_p + t_n + f_p + f_n} \dots (10)$$

$$d = \frac{1}{N}\sum_{i=1}^{N} t_{en\ i} - t_{star\ i} \dots (11)$$

Where, $t_p, f_p, t_n \& f_n$ are constants of confusion matrix, while $t_{end} \& t_{start}$ are the timestamps of completing and starting the classification process. These metrics were estimated on the following dataset samples,

- Fabric defect data samples (https://www.kaggle.com/datasets/rmshashi/fabric-defect-dataset)
- Textile defect detection samples (https://www.kaggle.com/datasets/belkhirnacim/textiledefectdetection)
- Fabric stain image samples (https://www.kaggle.com/datasets/priemshpathirana/fabric-stain-dataset)

These images were combined to form a total of 12500 image samples with 'Normal', 'Bad Selvage', 'Holes', 'Oil Spot', 'Thickness Defect', and 'Broken Ends' classes. These image sets were segregated into 80% training, 10% testing & 10% validation sample sets. Based on this strategy, the classification accuracy was estimated and compared with ALE CNN [3], SD CAE [8], and CNN [14] models w.r.t. Number of Sample Images (NSI) in table 1 as follows,

NSI	**A (%) ALE CNN [3]**	**A (%) SD CAE [8]**	**A (%) CNN [14]**	**A (%) MAC DCB**
554	81.21	88.48	85.81	97.69
1113	81.26	88.80	86.00	97.76
1667	81.31	89.11	86.18	97.82
2221	81.36	89.44	86.36	97.88
2779	81.41	89.77	86.56	97.92
3334	81.47	90.10	86.75	97.97
3888	81.52	90.43	86.95	98.00
4446	81.57	90.76	87.16	98.04

5000	81.62	91.08	87.36	98.09
5554	81.67	91.40	87.56	98.13
6113	81.72	91.72	87.76	98.19
6946	81.78	92.04	87.95	98.24
8334	81.83	92.37	88.14	98.31
9029	81.88	92.69	88.33	98.37
9721	81.93	93.01	88.52	98.42
11113	81.98	93.33	88.72	98.47
11804	82.04	93.66	88.91	98.52
12500	82.09	93.98	89.10	98.57

Table 1. Accuracy of cloth defect detection for different models

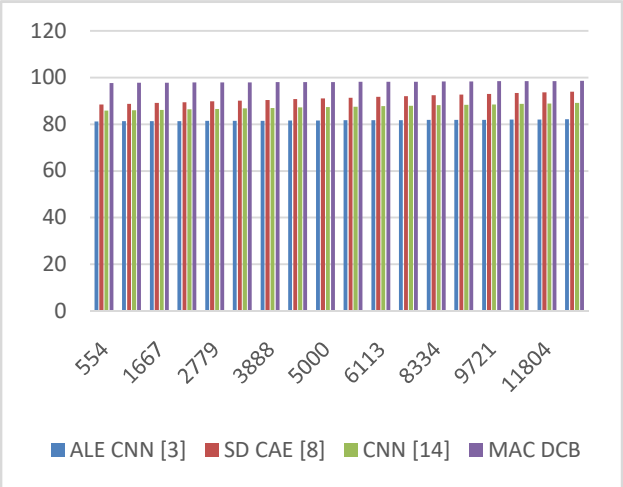

Fig 4. Accuracy of cloth defect detection for different models

As per this evaluation and **Fig** 4, it can be observed that the proposed cloth defect detection model is able to identify diseases with 16.5% more accuracy than ALE CNN [3], 4.3% higher accuracy than SD CAE [8], and 8.5% better accuracy than CNN [14] under real-time image sets. This accuracy is improved due to use of binary cascaded CNNs, which assists in optimizing the model's performance even under multiple defect types. Similarly, the precision levels can be observed from table 2 as follows,

NSI	P (%) ALE CNN [3]	P (%) SD CAE [8]	P (%) CNN [14]	P (%) MAC DCB
554	79.30	84.72	82.98	96.58
1113	79.35	85.03	83.16	96.63
1667	79.40	85.34	83.34	96.68
2221	79.46	85.66	83.52	96.73
2779	79.51	85.97	83.71	96.77
3334	79.56	86.29	83.90	96.81
3888	79.61	86.60	84.10	96.85
4446	79.66	86.90	84.29	96.90
5000	79.71	87.21	84.48	96.95
5554	79.76	87.51	84.67	97.00
6113	79.81	87.81	84.85	97.06
6946	79.86	88.12	85.04	97.12
8334	79.91	88.42	85.22	97.17
9029	79.96	88.73	85.40	97.23
9721	80.00	89.03	85.58	97.28
11113	80.06	89.34	85.77	97.33
11804	80.11	89.65	85.96	97.37
12500	80.16	89.97	86.15	97.42

Table 2. Precision of cloth defect detection for different models

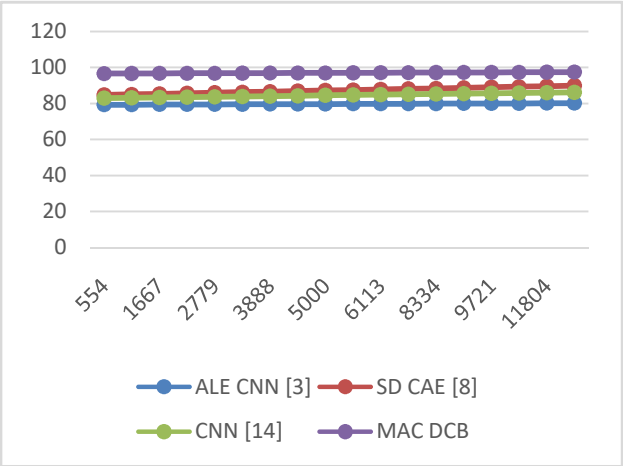

Fig 5. Precision of cloth defect detection for different models

As per this evaluation and **Fig** 5, it can be observed that the proposed cloth defect detection model is able to identify diseases with 15.9% more precision than ALE CNN [3], 8.5% higher precision than SD CAE [8], and 10.5% better precision than CNN [14] under real-time image sets. This precision is improved due to use of correlative augmentation with binary cascaded CNNs, which assists in optimizing the model's performance even under multiple defect types. Similarly, the recall levels can be observed from table 3 as follows,

NSI	**R (%) ALE CNN [3]**	**R (%) SD CAE [8]**	**R (%) CNN [14]**	**R (%) MAC DCB**
554	78.32	86.75	83.44	95.96
1113	78.37	87.07	83.62	96.02
1667	78.42	87.39	83.81	96.08
2221	78.48	87.70	83.99	96.13
2779	78.53	88.00	84.17	96.18
3334	78.60	88.28	84.36	96.23
3888	78.68	88.53	84.54	96.29
4446	78.77	88.77	84.71	96.36
5000	78.86	89.00	84.88	96.42
5554	78.95	89.23	85.05	96.50
6113	79.03	89.47	85.22	96.58

6946	79.11	89.72	85.40	96.65
8334	79.19	89.98	85.57	96.73
9029	79.26	90.24	85.74	96.80
9721	79.32	90.52	85.92	96.86
11113	79.39	90.81	86.10	96.92
11804	79.46	91.09	86.28	96.98
12500	79.53	91.36	86.46	97.04

Table 3. Recall of cloth defect detection for different models

As per this evaluation and **Fig** 6, it can be observed that the proposed cloth defect detection model is able to identify diseases with 18.3% more recall than ALE CNN [3], 5.9% higher recallthan SD CAE [8], and 10.3% better recallthan CNN [14] under real-time image sets. This recallis improved due to use of correlative augmentation with binary cascaded CNNs, which assists in optimizing the model's consistency even under multiple defect types. Similarly, the delay levels can be observed from table 4 as follows,

NSI	**D (ms) ALE CNN [3]**	**D (ms) SD CAE [8]**	**D (ms) CNN [14]**	**D (ms) MAC DCB**
554	111.45	103.98	100.90	93.29
1113	111.52	104.36	101.12	93.35
1667	111.60	104.74	101.33	93.40
2221	111.67	105.12	101.56	93.45
2779	111.74	105.51	101.78	93.49
3334	111.81	105.90	102.01	93.53
3888	111.88	106.28	102.24	93.57
4446	111.95	106.66	102.48	93.61
5000	112.02	107.04	102.71	93.65
5554	112.10	107.42	102.94	93.70
6113	112.17	107.79	103.17	93.75

6946	112.24	108.16	103.40	93.81
8334	112.31	108.54	103.62	93.87
9029	112.38	108.91	103.85	93.92
9721	112.45	109.29	104.07	93.97
11113	112.52	109.68	104.30	94.02
11804	112.59	110.06	104.53	94.06
12500	112.66	110.44	104.75	94.11

Table 4. Delay of cloth defect detection for different models

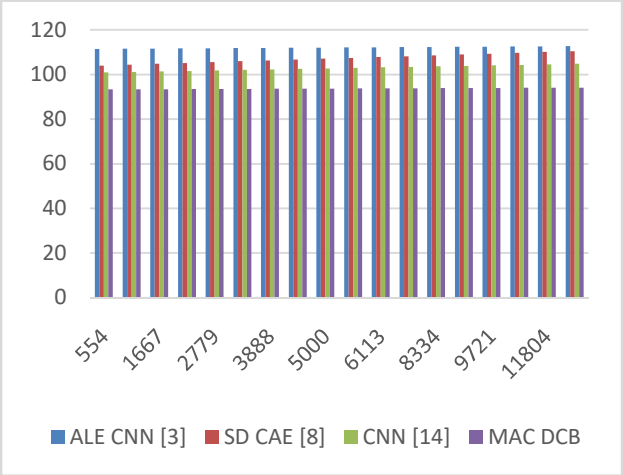

Fig 7. Delay of cloth defect detection for different models

As per this evaluation and **Fig** 7, it can be observed that the proposed cloth defect detection model is able to identify diseases with 19.5% lower delay than ALE CNN [3], 10.8% lower delaythan SD CAE [8], and 8.3% lower delaythan CNN [14] under real-time image sets. This speed is improved due to use of correlative augmentation with binary cascaded CNNs, which assists in optimizing the model's speed even under multiple defect types. Due to these optimizations, the proposed model is able to identify cloth defects with higher performance even under higher number of defect types under real-time scenarios.

4. Conclusion and Future Scope

The suggested model first gathers fabric pictures from various fault classes before enhancing them using a correlation procedure. This correlation approach aids in the detection of class-level picture sets with extremely low correlation. A binary cascaded CNN method classifies these picture sets into 1 of N fault categories. Using binary classification, the model can predict defect classes with high levels of accuracy. In terms of accuracy, it was shown that the suggested fabric defect detection model can diagnose illnesses with 16.5% greater accuracy than ALE CNN [3], 4.3% higher accuracy than SD CAE [8, and 8.5% better accuracy than CNN [14] when using real-time picture sets. Utilizing binary cascaded CNNs aids in improving the model's performance even in the presence of various fault kinds, hence enhancing its accuracy. In terms of consistency, it was determined that the suggested fabric defect detection model is capable of identifying illnesses with 15.9% greater accuracy than ALE CNN [3], 8.5% higher precision than SD CAE [8], and 10.0% better precision than CNN [14] when using real-time picture sets. This accuracy is enhanced by the use of correlative augmentation using binary cascaded CNNs, which aids in improving the model's performance even when

numerous fault kinds are present. In terms of scalability, it was shown that the suggested cloth defect detection model can identify illnesses with 18.3% greater recall than ALE CNN [3], 5.9% higher recall than SD CAE [8], and 10.0% better recall than CNN [14] using real-time picture sets. This recall is enhanced by the use of correlative augmentation using binary cascaded CNNs, which aids in maximizing the model's consistency even in the presence of several defect kinds. In terms of classification speed, it was shown that the suggested fabric defect detection model can identify illnesses with 19.5% less delay than ALE CNN [3], 10.8% less delay than SD CAE [8], and 8.3% less delay than CNN [14] using real-time picture sets. The use of correlative augmentation with binary cascaded CNNs helps to optimize the model's performance even in the presence of many fault kinds. Due to these changes, the suggested model is able to recognize fabric flaws with improved efficiency, even in real-time settings with a greater number of defect kinds.

In the future, it will be necessary to assess the suggested model on bigger picture sets, and it may be enhanced by the incorporation of Q-Learning, Generative Adversarial Networks (GANs), and other transformer models. This performance may also be enhanced by using hybrid bioinspired strategies for feature selection and contextual segmentation algorithms for fault localization via deep learning processes.

References

[1] D. Mo, W. K. Wong, Z. Lai and J. Zhou, "Weighted Double-Low-Rank Decomposition With Application to Fabric Defect Detection," in IEEE Transactions on Automation Science and Engineering, vol. 18, no. 3, pp. 1170-1190, July 2021, doi: 10.1109/TASE.2020.2997718.

[2] W. Wang, N. Deng and B. Xin, "Sequential Detection of Image Defects for Patterned Fabrics," in IEEE Access, vol. 8, pp. 174751-174762, 2020, doi: 10.1109/ACCESS.2020.3024695.

[3] W. Ouyang, B. Xu, J. Hou and X. Yuan, "Fabric Defect Detection Using Activation Layer Embedded Convolutional Neural Network," in IEEE Access, vol. 7, pp. 70130-70140, 2019, doi: 10.1109/ACCESS.2019.2913620.

[4] B. Lu, M. Zhang and B. Huang, "Deep Adversarial Data Augmentation for Fabric Defect Classification With Scarce Defect Data," in IEEE Transactions on Instrumentation and Measurement, vol. 71, pp. 1-13, 2022, Art no. 5014613, doi: 10.1109/TIM.2022.3185609.

[5] L. Shao, E. Zhang, Q. Ma and M. Li, "Pixel-Wise Semisupervised Fabric Defect Detection Method Combined With Multitask Mean Teacher," in IEEE Transactions on Instrumentation and Measurement, vol. 71, pp. 1-11, 2022, Art no. 2506011, doi: 10.1109/TIM.2022.3162286.

[6] Z. Wang and J. Jing, "Pixel-Wise Fabric Defect Detection by CNNs Without Labeled Training Data," in IEEE Access, vol. 8, pp. 161317-161325, 2020, doi: 10.1109/ACCESS.2020.3021189.

[7] H. Xie, Y. Zhang and Z. Wu, "Fabric Defect Detection Method Combing Image Pyramid and Direction Template," in IEEE Access, vol. 7, pp. 182320-182334, 2019, doi: 10.1109/ACCESS.2019.2959880.

[8] C. Li, G. Gao, Z. Liu, D. Huang and J. Xi, "Defect Detection for Patterned Fabric Images Based on GHOG and Low-Rank Decomposition," in IEEE Access, vol. 7, pp. 83962-83973, 2019, doi: 10.1109/ACCESS.2019.2925196.

[9] Y. Huang, J. Jing and Z. Wang, "Fabric Defect Segmentation Method Based on Deep Learning," in IEEE Transactions on Instrumentation and Measurement, vol. 70, pp. 1-15, 2021, Art no. 5005715, doi: 10.1109/TIM.2020.3047190.

[10] L. Song, R. Li and S. Chen, "Fabric Defect Detection Based on Membership Degree of Regions," in IEEE Access, vol. 8, pp. 48752-48760, 2020, doi: 10.1109/ACCESS.2020.2978900.

[11] M. M. Khodier, S. M. Ahmed and M. S. Sayed, "Complex Pattern Jacquard Fabrics Defect Detection Using Convolutional Neural Networks and Multispectral Imaging," in IEEE Access, vol. 10, pp. 10653-10660, 2022, doi: 10.1109/ACCESS.2022.3144843.

[12] C. Zhang, S. Feng, X. Wang and Y. Wang, "ZJU-Leaper: A Benchmark Dataset for Fabric Defect Detection and a Comparative Study," in IEEE Transactions on Artificial Intelligence, vol. 1, no. 3, pp. 219-232, Dec. 2020, doi: 10.1109/TAI.2021.3057027.

[13] Z. Zhu, G. Han, G. Jia and L. Shu, "Modified DenseNet for Automatic Fabric Defect Detection With Edge Computing for Minimizing Latency," in IEEE Internet of Things Journal, vol. 7, no. 10, pp. 9623-9636, Oct. 2020, doi: 10.1109/JIOT.2020.2983050.

[14] Q. Liu, C. Wang, Y. Li, M. Gao and J. Li, "A Fabric Defect Detection Method Based on Deep Learning," in IEEE Access, vol. 10, pp. 4284-4296, 2022, doi: 10.1109/ACCESS.2021.3140118.

[15] T. Almeida, F. Moutinho and J. P. Matos-Carvalho, "Fabric Defect Detection With Deep Learning and False Negative Reduction," in IEEE Access, vol. 9, pp. 81936-81945, 2021, doi: 10.1109/ACCESS.2021.3086028.

[16] J. Liu, C. Wang, H. Su, B. Du and D. Tao, "Multistage GAN for Fabric Defect Detection," in IEEE Transactions on Image Processing, vol. 29, pp. 3388-3400, 2020, doi: 10.1109/TIP.2019.2959741.

[17] Y. Dong, J. Wang, C. Li, Z. Liu, J. Xi and A. Zhang, "Fusing Multilevel Deep Features for Fabric Defect Detection Based NTV-RPCA," in IEEE Access, vol. 8, pp. 161872-161883, 2020, doi: 10.1109/ACCESS.2020.3021482.

[18] B. Fang, X. Long, F. Sun, H. Liu, S. Zhang and C. Fang, "Tactile-Based Fabric Defect Detection Using Convolutional Neural Network With Attention Mechanism," in IEEE Transactions on Instrumentation and Measurement, vol. 71, pp. 1-9, 2022, Art no. 5011309, doi: 10.1109/TIM.2022.3165254.

[19] B. Shi, J. Liang, L. Di, C. Chen and Z. Hou, "Fabric Defect Detection via Low-Rank Decomposition With Gradient Information," in IEEE Access, vol. 7, pp. 130423-130437, 2019, doi: 10.1109/ACCESS.2019.2939843.

[20] R. A. Lizarraga-Morales, F. E. Correa-Tome, R. E. Sanchez-Yanez and J. Cepeda-Negrete, "On the Use of Binary Features in a Rule-Based Approach for Defect Detection on Patterned Textiles," in IEEE Access, vol. 7, pp. 18042-18049, 2019, doi: 10.1109/ACCESS.2019.2896078.

[21] M. Kim, H. Jo, M. Ra and W. -Y. Kim, "Weakly-Supervised Defect Segmentation on Periodic Textures Using CycleGAN," in IEEE Access, vol. 8, pp. 176202-176216, 2020, doi: 10.1109/ACCESS.2020.3024554.

[22] Z. Zeng, B. Liu, J. Fu and H. Chao, "Reference-Based Defect Detection Network," in IEEE Transactions on Image Processing, vol. 30, pp. 6637-6647, 2021, doi: 10.1109/TIP.2021.3096067.
[23] Y. Moradi, M. Ibrahim, K. Chakrabarty and U. Schlichtmann, "An Efficient Fault-Tolerant Valve-Based Microfluidic Routing Fabric for Droplet Barcoding in Single-Cell Analysis," in IEEE Transactions on Computer-Aided Design of Integrated Circuits and Systems, vol. 39, no. 2, pp. 359-372, Feb. 2020, doi: 10.1109/TCAD.2018.2889765.
[24] W. F. Halawa, S. M. Darwish and A. A. Elzoghabi, "Cotton Warehousing Improvement for Bale Management System Based on Neutrosophic Classifier," in IEEE Access, vol. 9, pp. 159413-159420, 2021, doi: 10.1109/ACCESS.2021.3126790.
[25] Z. Liu, W. Lyu, C. Wang, Q. Guo, D. Zhou and W. Xu, "D-CenterNet: An Anchor-Free Detector With Knowledge Distillation for Industrial Defect Detection," in IEEE Transactions on Instrumentation and Measurement, vol. 71, pp. 1-12, 2022, Art no. 2518412, doi: 10.1109/TIM.2022.3204332.
[26] R. Wang, Q. Guo, S. Lu and C. Zhang, "Tire Defect Detection Using Fully Convolutional Network," in IEEE Access, vol. 7, pp. 43502-43510, 2019, doi: 10.1109/ACCESS.2019.2908483.
[27] Y. Gao, L. Gao, X. Li and X. V. Wang, "A Multilevel Information Fusion-Based Deep Learning Method for Vision-Based Defect Recognition," in IEEE Transactions on Instrumentation and Measurement, vol. 69, no. 7, pp. 3980-3991, July 2020, doi: 10.1109/TIM.2019.2947800.
[28] X. Yu, W. Lyu, D. Zhou, C. Wang and W. Xu, "ES-Net: Efficient Scale-Aware Network for Tiny Defect Detection," in IEEE Transactions on Instrumentation and Measurement, vol. 71, pp. 1-14, 2022, Art no. 3511314, doi: 10.1109/TIM.2022.3168897.
[29] H. Yang, Y. Chen, K. Song and Z. Yin, "Multiscale Feature-Clustering-Based Fully Convolutional Autoencoder for Fast Accurate Visual Inspection of Texture Surface Defects," in IEEE Transactions on Automation Science and Engineering, vol. 16, no. 3, pp. 1450-1467, July 2019, doi: 10.1109/TASE.2018.2886031.
[30] D. Xu, B. Lu and B. Huang, "A Multiscale Convolutional Registration Network for Defect Inspection on Periodic Lace Surfaces," in IEEE Transactions on Instrumentation and Measurement, vol. 71, pp. 1-9, 2022, Art no. 5006009, doi: 10.1109/TIM.2022.3150581.
[31] E. Ozen and A. Orailoglu, "Architecting Decentralization and Customizability in DNN Accelerators for Hardware Defect Adaptation," in IEEE Transactions on Computer-Aided Design of Integrated Circuits and Systems, vol. 41, no. 11, pp. 3934-3945, Nov. 2022, doi: 10.1109/TCAD.2022.3197540.
[32] B. Feng, D. J. Pasadas, A. L. Ribeiro and H. G. Ramos, "Locating Defects in Anisotropic CFRP Plates Using ToF-Based Probability Matrix and Neural Networks," in IEEE Transactions on Instrumentation and Measurement, vol. 68, no. 5, pp. 1252-1260, May 2019, doi: 10.1109/TIM.2019.2893701.